Geophys. J. R. astr. Soc. (1984) 79, 89–104

Paraxial ray approximations in the computation of seismic wavefields in inhomogeneous media

V. Červený and L. Klimeš *Institute of Geophysics, Charles University, Ke Karlovu 3, 121 16 Praha 2, Czechoslovakia*

I. Pšenčík *Geophysical Institute, Czechoslovak Academy of Science, Boční II, 141 31 Praha 4, Czechoslovakia*

Accepted, in revised form, 1984 January 21

Summary. Several important applications of the paraxial ray approximation (PRA) to numerical modelling of high-frequency seismic body wavefields are discussed. The PRA can be used to evaluate the displacement vector not only directly on the ray, as in the standard ray method, but also approximately in the vicinity of this ray. The PRA also offers simple ways of approximate evaluation of paraxial rays, situated in the vicinity of the central ray, and of two-point ray tracing. A very important application of the PRA consists in a simple, fast and effective computation of body-wave synthetic seismograms in general, 3-D, laterally inhomogeneous, layered structures. Examples of synthetic seismograms for 3-D structures, computed using the PRA, are presented.

1 Introduction

In the paraxial ray approximation (PRA), a particular ray is taken to be the coordinate axis of the so-called ray-centred coordinate system. We refer to this ray as the central ray Ω and evaluate approximately the wavefield in the vicinity of the central ray (i.e. in the vicinity of the coordinate axis), not just on the ray as in the standard ray method. This is the reason why this approach is called the *paraxial ray approximation.* The wavefield at any point in the vicinity of the central ray can be computed directly from quantities determined along the central ray by the procedure called *dynamic ray tracing.* It is not necessary to seek another ray, which passes through the point, by time-consuming two-point ray tracing.

Dynamic ray tracing and the PRA offer the following possibilities:

(a) simple computation of geometrical spreading with simple determination of phase shift due to caustics along the central ray Ω;

(b) determination of the second derivatives of the travel-time field and of the curvatures of the wavefront along the central ray Ω;

(c) simple and fast initial-value as well as two-point ray tracing of paraxial rays (rays situated in the vicinity of a known central ray);

(d) approximate evaluation of the displacement vector at any point situated in the close vicinity of the central ray;

(e) fast and effective computation of body-wave synthetic seismograms in general, 2-D and 3-D, laterally varying, layered structures;

(f) simple evaluation of certain quantities needed in the Gaussian beam approach and in the Maslov asymptotic theory.

Notice the close connection between the PRA and the equations describing high-frequency elastodynamic Gaussian beams and the equations of the Maslov asymptotic theory. In fact, the PRA represents the limiting case of a Gaussian beam. In this limit, the PRA corresponds to an infinitely wide Gaussian beam. Moreover, by an integral superposition of paraxial ray approximations connected with rays forming an orthonomic system of rays we can obtain a solution of the elastodynamic equations which removes certain singularities of the ray method, for details refer to Červený (1983), and Červený & Klimeš (1984). An individual paraxial ray approximation, however, does not remove ray singularities, such as sharp boundaries between shadow and illuminated zones.

In this paper, we shall mostly concentrate on the problems connected with items (c), (d) and (e) given above. We shall also briefly describe the computer program designed for the evaluation of body-wave synthetic seismograms in general, laterally varying, 3-D, layered structures based on the PRA, and present examples of computations.

We shall consider an isotropic perfectly elastic 3-D model of a medium composed of laterally inhomogeneous layers separated by curved interfaces. The surface of the model may be curved too. The velocity and density distributions in the individual layers are described by smooth functions $v_P(x_i)$, $v_S(x_i)$, $\rho(x_i)$ of general Cartesian coordinates x_i.

Note that we use two types of suffix throughout the paper. Lower case suffices, such as $i, j, k, l \ldots$ take the values 1, 2, 3, while capital letters, such as $I, J, K, L \ldots$ only take the values 1, 2. The Einstein summation convention is used in both cases.

2 Ray-centred coordinates and dynamic ray tracing

Let us consider an orthonomic two-parametric system of rays and denote the ray parameters by γ_1, γ_2.

2.1 COMPUTATION OF RAYS

As in the standard ray method, the basic step in evaluating the seismic wavefield using PRA consists in initial-value (Cauchy) ray tracing, which is a simple problem even in 3-D media. We consider the ray tracing system in the form of

$$\frac{dx_i}{d\sigma} = p_i, \qquad \frac{dp_i}{d\sigma} = -v^{-3}\,\frac{\partial v}{\partial x_i}, \tag{1}$$

where σ is the parameter measured along the ray. It is related to the travel time τ and to the arclength s by

$$\sigma = \sigma_0 + \int_{s_0}^{s} v\,ds = \sigma_0 + \int_{\tau_0}^{\tau} v^2\,d\tau. \tag{2}$$

The quantity $v = v(x_i)$ denotes the velocity of propagation of the corresponding type of wave (it equals either v_P or v_S). Quantities x_i in (1) are Cartesian coordinates of points of a ray and $p_i = \partial\tau/\partial x_i$ are Cartesian components of the slowness vector. We shall denote $\gamma_3 = \sigma$ and use $\gamma_i \equiv (\gamma_1, \gamma_2, \gamma_3)$ as the ray coordinates.

The initial conditions for solving the ray tracing system (1) must satisfy the eikonal equation $p_i p_i = v^{-2}$. The solutions of the ray tracing system (1) then satisfy the eikonal equation along the whole ray. This may be used to check the numerical accuracy of the ray tracing.

2.2 RAY-CENTRED COORDINATE SYSTEM

The orthogonal ray-centred coordinate system along a selected ray Ω and its computation is described in Popov & Pšenčík (1978), Pšenčík (1979), Červený & Hron (1980). We shall denote the ray-centred coordinates connected with Ω by $q_i = (q_1, q_2, q_3 = s)$, where s is the arclength along Ω and q_I are the Cartesian coordinates in the plane perpendicular to Ω at a point $s = q_3$ with the origin on Ω.

The vector basis of the ray-centred coordinate system consists of three unit vectors $\mathbf{e}_1, \mathbf{e}_2$, $\mathbf{t}$, where $\mathbf{t}$ is tangent to the ray and vectors $\mathbf{e}_1, \mathbf{e}_2$ are perpendicular to the ray. They are introduced in such a way as to render the ray-centred coordinate system orthogonal. Note that the columns of the unitary transformation matrix

$$H_{ij} = \left.\frac{\partial x_i}{\partial q_j}\right|_{q_K=0} = \left.\frac{\partial q_j}{\partial x_i}\right|_{q_K=0} \tag{3}$$

are constituted of the basis vectors $\mathbf{e}_1, \mathbf{e}_2, \mathbf{t}$ expressed in general Cartesian coordinates x_i.

The vector basis of the ray-centred coordinate system (particularly the vectors $\mathbf{e}_1, \mathbf{e}_2$) also determines the polarization of the displacement vector of S-waves. In the ray-centred coordinate system, the displacement vector does not rotate with respect to the coordinate axes, but translates parallelly along the ray.

2.3 DYNAMIC RAY TRACING

The principle role of the PRA is played by the system of ordinary differential equations for the components of a 4×1 column matrix $\mathbf{W}(\sigma)$,

$$\frac{d\mathbf{W}(\sigma)}{d\sigma} = \mathbf{S}(\sigma)\mathbf{W}(\sigma), \tag{4}$$

where $\mathbf{S}(\sigma)$ is a 4×4 matrix

$$\mathbf{S}(\sigma) = \begin{pmatrix} \mathbf{O} & \mathbf{I} \\ -v^{-3}(\sigma)\mathbf{V}(\sigma) & \mathbf{O} \end{pmatrix}, \tag{5}$$

$\mathbf{O}$ and $\mathbf{I}$ being 2×2 null and identity matrices. The elements of the 2×2 matrix $\mathbf{V}(\sigma)$ are given as

$$V_{IJ}(\sigma) = \left.\frac{\partial^2 v}{\partial q_I \partial q_J}\right|_{q_M=0} = H_{kI}H_{lJ}\left.\frac{\partial^2 v}{\partial x_k \partial x_l}\right|_{q_M=0}. \tag{6}$$

The system (4), here called the dynamic ray tracing system, has four linearly independent solutions. We denote by $\pi(\sigma_1 \sigma_0)$ the fundamental 4×4 matrix of linearly independent solutions of (4), specified at $\sigma = \sigma_0$ by $\pi(\sigma_0, \sigma_0) = \mathbf{I}$, where $\mathbf{I}$ is now a 4×4 identity matrix. Any solution of (4) can be expressed in the form

$$\mathbf{W}(\sigma) = \pi(\sigma, \sigma_0)\mathbf{W}(\sigma_0) \tag{7}$$

with $\mathbf{W}(\sigma_0)$ specified.

In the PRA, of basic importance is the 4×2 matrix $\mathbf{X}(\sigma)$, the columns of which are

formed by the solutions of (4). We express $\mathbf{X}(\sigma)$ in terms of 2 x 2 matrices $\mathbf{Q}(\sigma)$ and $\mathbf{P}(\sigma)$,

$$\mathbf{X}(\sigma) = \begin{pmatrix} \mathbf{Q}(\sigma) \\ \mathbf{P}(\sigma) \end{pmatrix}. \tag{8}$$

If the matrices $\mathbf{Q}(\sigma)$ and $\mathbf{P}(\sigma)$ satisfy the relations

$$Q_{IJ} = \frac{\partial q_I}{\partial \gamma_J}\bigg|_{q_M = 0}, \qquad P_{IJ} = \frac{\partial^2 \tau}{\partial \gamma_J \, \partial q_I}\bigg|_{q_M = 0} \tag{9}$$

at an arbitrary point $\sigma = \sigma_0$ of the ray, they satisfy the relations (9) along the whole ray. The matrix $\mathbf{Q}$ given by (9) is the transformation matrix from the ray coordinates γ_I to the ray-centred coordinates q_I. Note that the geometrical spreading is proportional to the quantity $|\det(\mathbf{Q})|^{1/2}$, so that matrix $\mathbf{Q}$ is also very useful in the evaluation of standard ray amplitudes.

The matrix

$$\mathbf{M} = \mathbf{P}\mathbf{Q}^{-1}, \tag{10}$$

formed by matrices (9), represents the matrix of the second derivatives of the travel-time field

$$M_{IJ} = \frac{\partial^2 \tau}{\partial q_I \, \partial q_J}\bigg|_{q_M = 0}. \tag{11}$$

It is related to the wavefront curvature matrix $\mathbf{K}$ by the formula $\mathbf{K} = v\mathbf{M}$.

If we know the fundamental matrix $\pi(\sigma, \sigma_0)$, we can simply evaluate the matrix $\mathbf{X}(\sigma)$ as

$$\mathbf{X}(\sigma) = \pi(\sigma, \sigma_0)\,\mathbf{X}(\sigma_0) \tag{12}$$

for any $\mathbf{X}(\sigma_0)$ which is here called the matrix of the initial parameters of the PRA. For instance, at a point source $\mathbf{X}(\sigma_0) = \begin{pmatrix} \mathbf{O} \\ \mathbf{P}(\sigma_0) \end{pmatrix}$, $\mathbf{O}$ being a 2 x 2 null matrix.

In a layered medium, the matrices $\mathbf{Q}$ and $\mathbf{P}$ and, consequently, $\mathbf{M}$ must be transformed across interfaces. The relevant transformation expressions can be deduced from those given by Popov & Pšenčík (1978), Hubral (1979), Červený & Hron (1980), etc.

3 Paraxial ray solutions in the vicinity of a specified point of the central ray

Equations for an approximate evaluation of the displacement vector at any point S situated in the close vicinity of the central ray Ω, were derived in Červený & Pšenčík (1983). The position of S was specified in ray-centred coordinates connected with Ω. To apply the formulae, certain quantities (among them the results of dynamic ray tracing) had to be known at point S_0, which is a projection of S on the ray Ω.

In many practical applications, however, we do not know the above quantities at point S_0, but at some different point Q of Ω, situated in some vicinity of S_0. Moreover, the coordinates of point S are usually specified in Cartesian coordinates, not in ray-centred coordinates. As an example of points Q and S we can consider the termination point of a ray and a receiver, both situated at the Earth's surface. The determination of points S_0 for different rays could be an expensive procedure, requiring all rays under consideration to be stored in a computer.

Here we shall present alternative expressions which can be used to evaluate the displacement vector at point S when the relevant quantities are known at some point Q on the ray Ω. We assume that the positions of both S and Q are specified in Cartesian coordinates. The

expressions are valid when point S is close to point Q, or more specifically, when point S is situated in the effective vicinity of point Q. By the effective vicinity of point Q we understand a spherical region with its centre at Q and with the radius $r = 0(\omega^{-1/2})$, for $\omega \to \infty$.

The presented equations can be derived by expanding the expressions given in Červený & Pšenčík (1983) in the effective vicinity of Q and transforming the resulting expressions into the appropriate coordinate system. For the 2-D case, this procedure was used in Červený & Pšenčík (1984), for comparison see also similar expansion in Klimeš (1984).

For simplicity, the effects of reflection and transmission are not considered in the following equations. The modification of the equations required to include these effects presents no difficulties and will be described elsewhere.

We denote by A_i the components of the vectorial complex-valued ray amplitude in the ray-centred coordinate system, taken directly on the central ray, $\mathbf{A} = A_1\mathbf{e}_1 + A_2\mathbf{e}_2 + A_3\mathbf{t}$,

$$A_i(\sigma) = \Phi_i[\rho(\sigma)v(\sigma)|\det \mathbf{Q}(\sigma)|]^{-1/2} \exp[i\phi(\sigma, \sigma_0)]. \tag{13}$$

The generally complex-valued factors Φ_i are constant along the ray and some of them are zero, $\Phi_I = 0$ for P-waves, $\Phi_3 = 0$ for S-waves. The quantity v denotes the velocity of propagation of the corresponding type of wave, ρ is the density, $|\det \mathbf{Q}(\sigma)|^{1/2}$ is proportional to the geometrical spreading, $\phi(\sigma, \sigma_0) = -(\pi/2)$ KMAH is the phase shift between points σ_0 and σ due to caustics (see the KMAH index in Chapman & Drummond 1982). The phase shift can be simply checked using the matrix $\mathbf{Q}(\sigma)$. Note that σ_0 denotes an arbitrary reference point on the ray, at which the constants Φ_i are specified.

The final expressions for the Cartesian components of the displacement vector at point $S(x_i)$, using the PRA in the effective vicinity of point $Q(x_i)$, read as follows

$$u_i(S, \omega) = a_i(S, Q) \exp[i\omega T(S, Q)], \tag{14}$$

with

$$T(S, Q) = \tau(Q) + x_j(S, Q)p_j(Q) + \tfrac{1}{2}x_j(S, Q)x_k(S, Q)H_{jm}(Q)H_{kn}(Q)M_{mn}(Q). \tag{15}$$

For P-waves

$$a_i(S, Q) = A_3(Q)[H_{i3}(Q) + v(Q)H_{iM}(Q)x_j(S, Q)H_{jn}(Q)M_{Mn}(Q)], \tag{16}$$

for S-waves

$$a_i(S, Q) = A_K(Q)[H_{iK}(Q) - v(Q)H_{i3}(Q)x_j(S, Q)H_{jn}(Q)M_{Kn}(Q)]. \tag{17}$$

The first terms on the rhs of (16) and (17) correspond to the principal components, the second terms correspond to the additional components. The following notation was used in (15)–(17):

$$x_i(S, Q) = x_i(S) - x_i(Q), \tag{18}$$

$$M_{ij} = \begin{pmatrix} M_{11} & M_{12} & -v^{-2}V_1 \\ M_{12} & M_{22} & -v^{-2}V_2 \\ -v^{-2}V_1 & -v^{-2}V_2 & -v^{-2}V_3 \end{pmatrix}, \tag{19}$$

where

$$V_i = \frac{\partial v}{\partial q_i}\bigg|_{q_M = 0} = H_{ji}\frac{\partial v}{\partial x_j}\bigg|_{q_M = 0} \tag{20}$$

is the velocity gradient in the ray-centred coordiate system. The matrix H_{ij} is given by (3).

Using the above expressions, we can evaluate the wavefield at any point S on the Earth's surface from the quantities A_i, τ, $\mathbf{Q}$, $\mathbf{P}$ (and thus $\mathbf{M}$), H_{ij}, v, V_i, ρ determined at the closest termination point of a ray at the Earth's surface. We neither need to store these quantities along the ray, nor to determine the corresponding projection of S on the ray.

4 Paraxial rays and two-point ray tracing

Another important application of the dynamic ray tracing is the approximate tracing of rays, so-called paraxial rays, in a close vicinity of the central ray. We can consider either initial-value (Cauchy) ray tracing or two-point ray tracing.

4.1 APPROXIMATE INITIAL-VALUE TRACING OF PARAXIAL RAYS

It is possible to show that the components of the 4×1 column matrix $\mathbf{W}(\sigma) = [q_1(\sigma), q_2(\sigma), p_1(\sigma), p_2(\sigma)]^T$, given by (7), are approximately the ray-centred coordinates and the components of the slowness vector in the ray-centred coordinate system, corresponding to the paraxial ray starting from point $q_1(\sigma_0), q_2(\sigma_0)$ with the slowness vector components $p_1(\sigma_0)$, $p_2(\sigma_0)$ as expressed in the ray-centred coordinate system.

Thus, in the vicinity of a known ray we do not need to perform standard ray tracing. Instead, we determine linearly independent solutions $\pi(\sigma, \sigma_0)$ of the dynamic ray tracing system (4). We can then determine approximately any paraxial ray with practically no additional effort, using (7) for different $\mathbf{W}(\sigma_0)$. The fundamental solutions $\pi(\sigma, \sigma_0)$ of (4) may, of course, be used simultaneously for some other purposes, e.g. for determining geometrical spreading, the curvature matrix, etc.

4.2 TWO-POINT RAY TRACING USING PARAXIAL RAYS

The paraxial rays described in Section 4.1 can be used very efficiently in two-point ray tracing which represents a rather complicated problem, especially in 3-D media. Here we consider quite general situation. We have two points A_1 and B_1 situated in the effective vicinities of some points A and B on a known ray Ω (see Fig. 1). We wish to determine the ray connecting the points A_1 and B_1 and the travel time between these points.

Assume that we have performed dynamic ray tracing from A to B. We thus know the fundamental matrix $\pi(B, A)$ (see Section 2.3) of solutions of the dynamic ray tracing system at point B. We introduce the following notations

$$\pi(B,A) = \begin{pmatrix} \pi_{11}(B,A) & \pi_{12}(B,A) \\ \pi_{21}(B,A) & \pi_{22}(B,A) \end{pmatrix}$$

$$\mathbf{Q}(B,A) = \pi_{12}(B,A),$$

$$\mathbf{M}(B,A) = \pi_{22}(B,A)\pi_{12}^{-1}(B,A), \qquad \mathbf{M}(A,B) = -\pi_{12}^{-1}(B,A)\pi_{11}(B,A),$$

$$M_{ij}(X,Y) = \begin{pmatrix} M_{11}(X,Y) & M_{12}(X,Y) & -v^{-2}(X)V_1(X) \\ M_{12}(X,Y) & M_{22}(X,Y) & -v^{-2}(X)V_2(X) \\ -v^{-2}(X)V_1(X) & -v^{-2}(X)V_2(X) & -v^{-2}(X)V_3(X) \end{pmatrix}, \tag{21}$$

where π_{IJ} are 2×2 submatrices of the fundamental matrix π. The velocity gradient V_i in the ray-centred coordinate system is given by (20). We denote by $p_i(A)$ the initial values of the Cartesian components of the slowness vector for ray tracing from A to B. Similarly, we

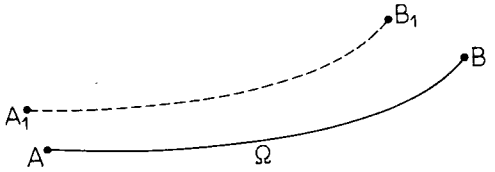

Figure 1. Two-point ray-tracing problem: find the ray connecting points A_1 and B_1 situated in the effective vicinities of points A and B on the known ray Ω.

denote by $p_i(B)$ the slowness vector at B corresponding to the ray from A to B. The approximate travel time from A_1 to B_1 is then

$$\tau(B_1, A_1) =$$
$$\tau(B, A) + x_i(B_1, B)p_i(B) - x_i(A_1, A)p_i(A) + \tfrac{1}{2}x_i(B_1, B)x_j(B_1, B)H_{ik}(B)H_{jl}(B)M_{kl}(B, A)$$
$$-\tfrac{1}{2}x_i(A_1, A)x_j(A_1, A)H_{ik}(A)H_{jl}(A)M_{kl}(A, B)$$
$$-x_i(A_1, A)x_j(B_1, B)H_{iK}(A)H_{jL}(B)Q^{-1}_{KL}(B, A), \tag{22}$$

where the matrix H_{ij} is given by (3), and $x_i(B_1, B) = x_i(B_1) - x_i(B)$ are the differences between the Cartesian coordinates of the points B_1 and B (see 18). The symbol Q^{-1}_{KL} denotes the element of matrix $\mathbf{Q}^{-1}$.

The initial values of the new slowness vector components of an approximate ray tracing from A_1 to B_1 can be obtained by differentiating (22) with respect to $x_i(A_1, A)$,

$$p_i(A_1) = -\frac{\partial\tau(B_1, A_1)}{\partial x_i(A_1, A)} = p_i(A) + H_{ik}(A)M_{kl}(A, B)H_{jl}(A)x_j(A_1, A)$$
$$+ H_{iK}(A)Q^{-1}_{KL}(B, A)H_{jL}(B)x_j(B_1, B). \tag{23}$$

We can now use $p_i(A_1)$, determined by (23), as the initial values for the standard ray tracing from A_1. Of course, the trajectory of the ray need not pass exactly through point B_1. It will, however, be closer to B_1 than ray Ω. If the distance between the new ray and point B_1 is not acceptable, the new ray may be considered as ray Ω and the above procedure may be repeated.

5 Application of the PRA to computing ray synthetic seismograms

The properties of the PRA discussed in Section 3 can be effectively used in the procedures of evaluating ray synthetic seismograms. The PRA replaces the time-consuming two-point ray tracing.

We consider here a point source situated at any point of a 3-D laterally varying layered structure, and a system of receivers, distributed in some region D_0 along the Earth's surface.

Similary as in the standard ray approach, the wavefield generated by a point source is computed as a superposition of elementary waves (reflected, refracted, converted, multiply reflected, etc.), corresponding to the zero-order approximation of the ray method.

The procedure for the computation of each elementary wave is the following:

(a) The first step is to compute a system of 3-D rays with termination points in region D_0. All the rays are computed from the source by initial-value ray tracing in different directions specified by ray parameters γ_1 and γ_2. The system of termination points must cover region D_0 with sufficient density. No two-point ray tracing is required and the receiver

coordinates need not be specified at this stage. Rays with termination points outside region D_0, on the side and bottom boundaries of the model, etc., need not be stored.

(b) Dynamic ray tracing is performed along all rays determined in (a). Dynamic ray tracing may be performed simultaneously with ray tracing, or immediately following it, if the ray is found to have a termination point in region D_0. All the necessary quantities at the termination points are stored. The rays themselves need not be stored for the subsequent computations.

(c) Using some criteria based mainly on comparisons of paraxial approximations corresponding to the individual termination points, the termination points appropriate to one elementary wave are sorted into groups corresponding to the individual branches of the travel-time field. Each group is then treated as an individual elementary wave. This sorting is necessary for elementary waves with several branches, e.g. the prograde and retrograde branches of refracted waves, etc.

The final result of the above three steps is a file containing several groups of data. Each group corresponds to one elementary wave (or to one branch of the elementary wave if the elementary wave has several branches). All the data, required to evaluate the wavefield in the vicinity of a particular termination point by the paraxial ray approximation, are stored in each group.

If such a file is available, the ray synthetic seismogram can be evaluated at any point of region D_0. Only now the coordinates of the receiver points distributed regularly or irregularly along various profiles, or individually, need to be specified. The profiles may be curved, piecewise linear, etc. Their orientation may, of course, be quite arbitrary.

Various variants of the PRA may be used for constructing impulse seismograms, i.e. for determining the travel time, ray amplitude and phase shift, at a specified receiver. The simplest way of determining these quantities at the receiver point is to use the PRA from the nearest termination point. Another possibility is to take a weighted superposition of the paraxial approximations corresponding to several of the closest termination points. The latter possibility is close to the approach based on the summation of Gaussian beams, see Klimeš (1984) and Červený & Klimeš (1984).

Once the impulse ray synthetic seismogram at the receiver point is known, it is easy to determine the ray seismogram corresponding to an arbitrary source-time function.

6 Program for computing 3-D ray synthetic seismograms: short description

The RD83 program was written to compute ray synthetic body wave seismograms in 3-D, inhomogeneous, laterally varying, layered structures. The PRA described in the preceding sections is used in the program. The displacement vector at any point of region D_0 on the Earth's surface is evaluated by the PRA from the nearest termination point, assuming that the distance to this point does not exceed a quantity ϵ specified in the input data. If there is no termination point in the ϵ-vicinity of the receiver, the receiver is considered to be situated in the shadow zone of the elementary wave under investigation (or of its branch). This means that the termination points must form the ϵ-network in the whole illuminated zone of region D_0. The density of termination points in the region D_0 can be checked in the plots of ray termination points, see, e.g. Fig. 3. If the density in some parts of the region D_0 is not sufficient, it is possible to try to trace some additional rays to those parts of D_0. Note that the quantity ϵ also specifies the possible error in determining the boundaries of shadow zones.

The RD83 program is composed of a set of interchangeable routines. Especially the routines describing the interfaces and velocity distribution within layers may be specified

by the user. At present, the most general routines for approximating the interfaces and velocity distribution used in RD83 have been taken from FITPACK by Cline (1981). The routine interpolate the 3-D velocity distribution specified at grid points of a rectangular network covering each layer by splines under tension. Similar routines are used to approximate the interfaces. The mentioned routines can be used to describe rather general 3-D models, although preparing the input data may be more involved for models with vanishing layers, etc. For models with non-intersecting interfaces the preparation of input data is simple.

At present, only a point source of *P*- and *S*-waves with isotropic distribution of complex-valued amplitudes over a unit sphere is used in the program.

The elements of rays between intersections with interfaces are computed by solving the ray tracing system (1) numerically. The system is solved simultaneously with the dynamic ray tracing system and with evaluating the vector base of the ray-centred coordinate system. Some routines transform all computed quantities across the interfaces. Other routines can sort the rays according to the branches of travel-time curves, compute elementary impulse seismograms at a given receiver point from the quantities stored at the termination points of rays, construct travel-time curves along specified profiles, etc. The profiles may be of any

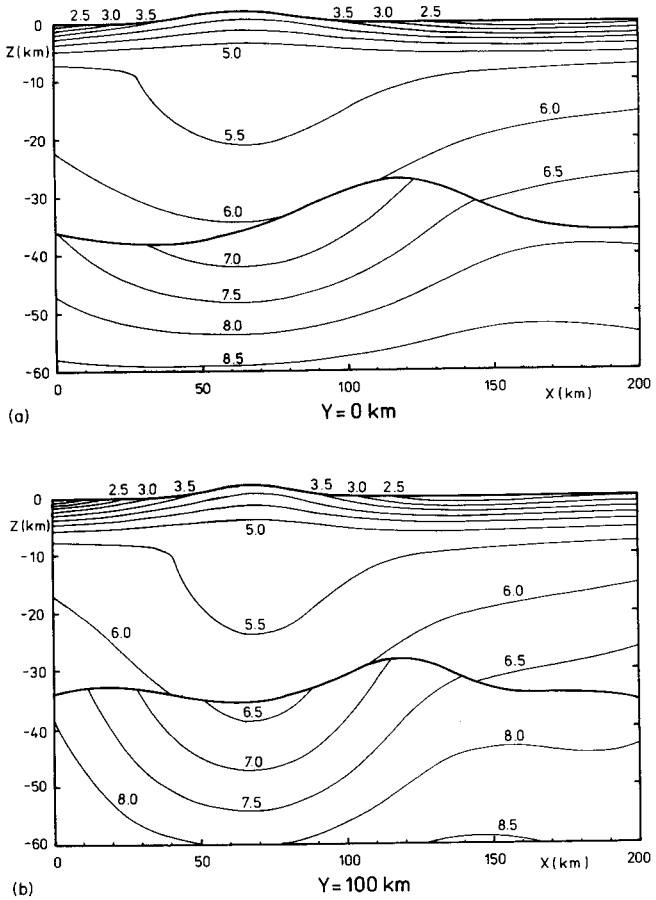

Figure 2. The 3-D model used for computing travel-time curves shown in Fig. 4 and synthetic seismograms shown in Fig. 5. Two vertical sections corresponding to planes $y = 0$ and 100 km are displayed. Thin lines with numbers denote the velocity isolines with the corresponding values of the wave velocity (in km s^{-1}), the bold line denotes the internal interface. The point source is situated at $x = y = z = 0$ km.

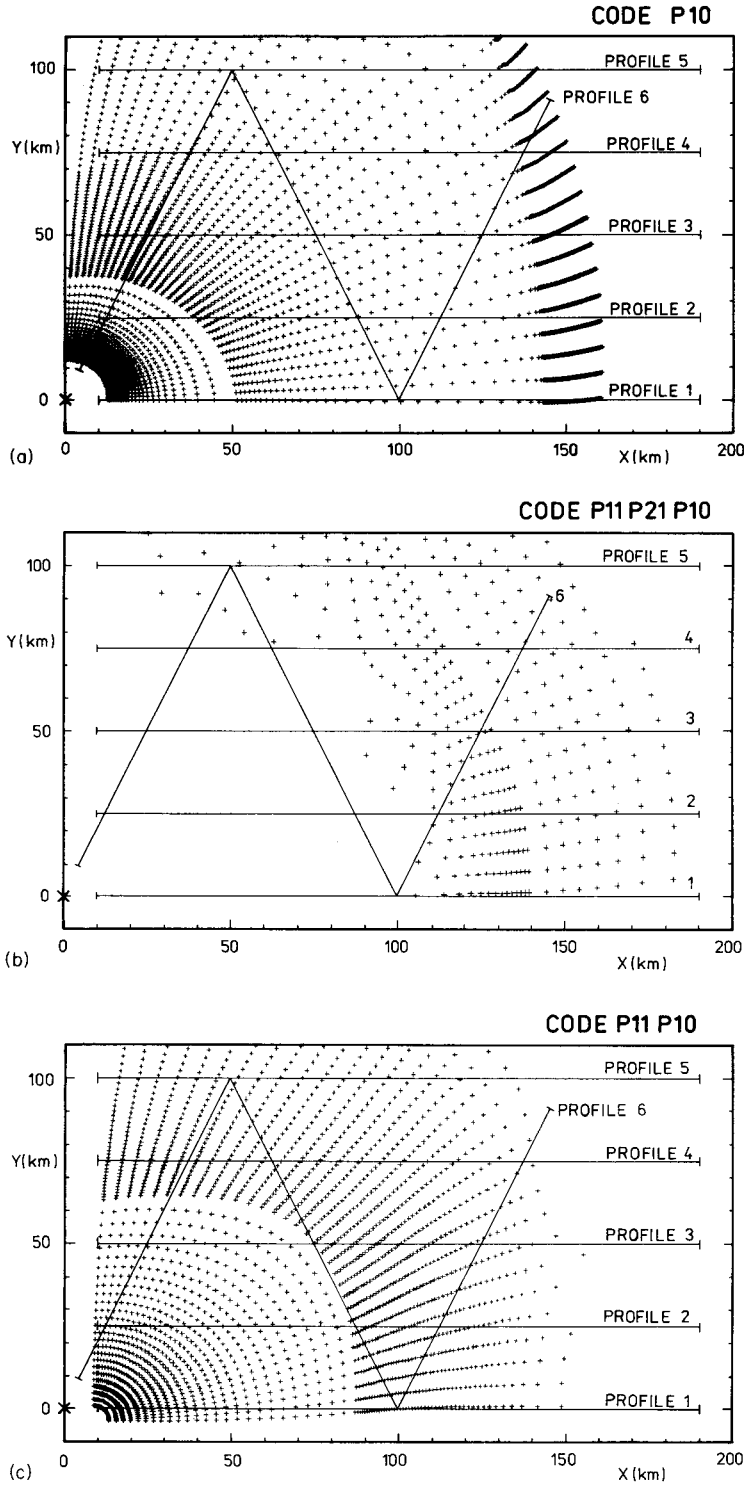

Figure 3. Ray termination points at the Earth's surface used for evaluating the synthetic seismograms shown in Fig. 5. The termination points correspond to the *P*-waves refracted in the upper layer ($P10$) and in the second layer ($P11P21P10$), and to the reflected *P*-wave ($P11P10$).

shape and need not contain the source. The SYSE program for constructing ray synthetic seismograms from stored impulse seismograms is an analogy of the SYNTPL and SEISPLOT programs adopted from the 2-D seismic ray package by Červený & Pšenčík (1981). In very much the same way as in SYNTPL and SEISPLOT, the source-time function (far-field approximation) is considered in the following form:

$$x(t) = \exp\left[-(2\pi f_0 t/\gamma)^2\right] \cos(2\pi f_0 t + \nu). \tag{24}$$

The first version of the RD83 program is described in details by Klimeš (1982).

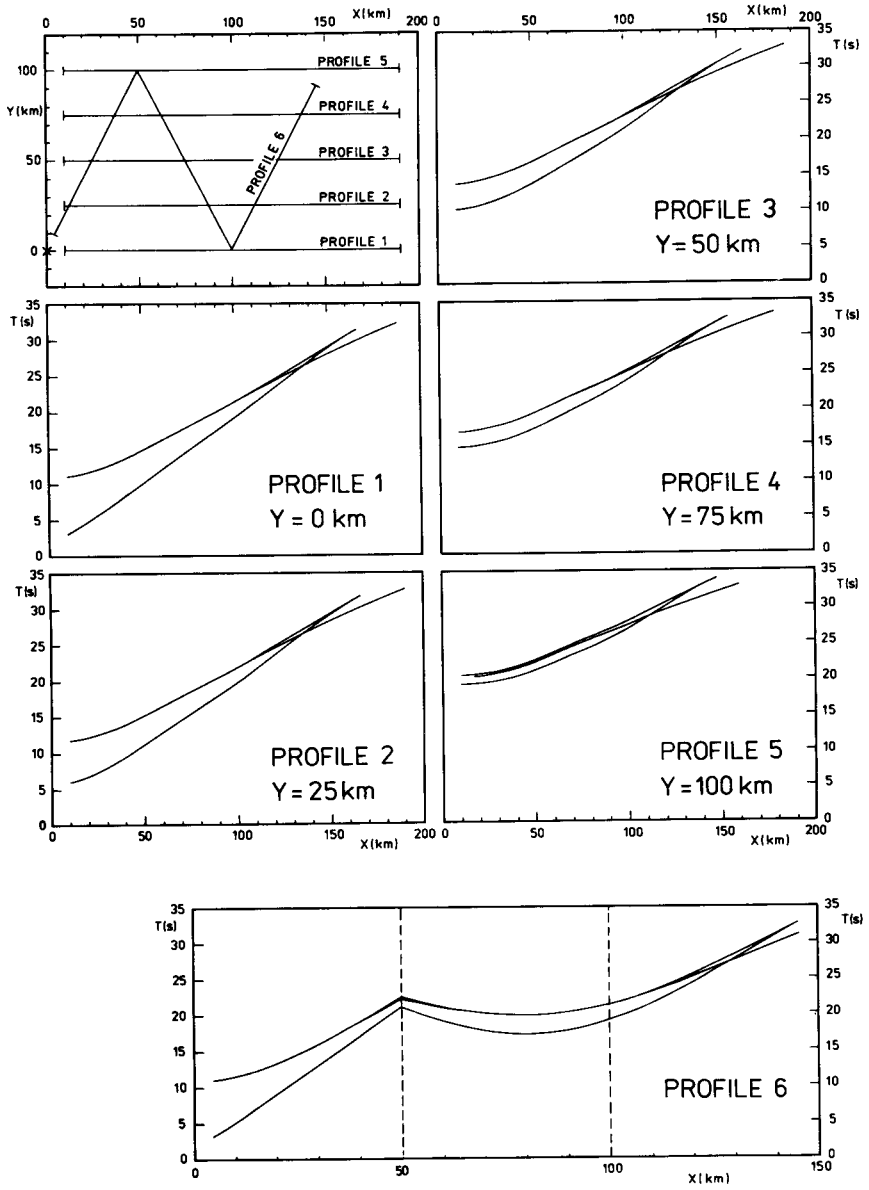

Figure 4. The positions of the profiles on the Earth's surface and the travel-time curves along these profiles.

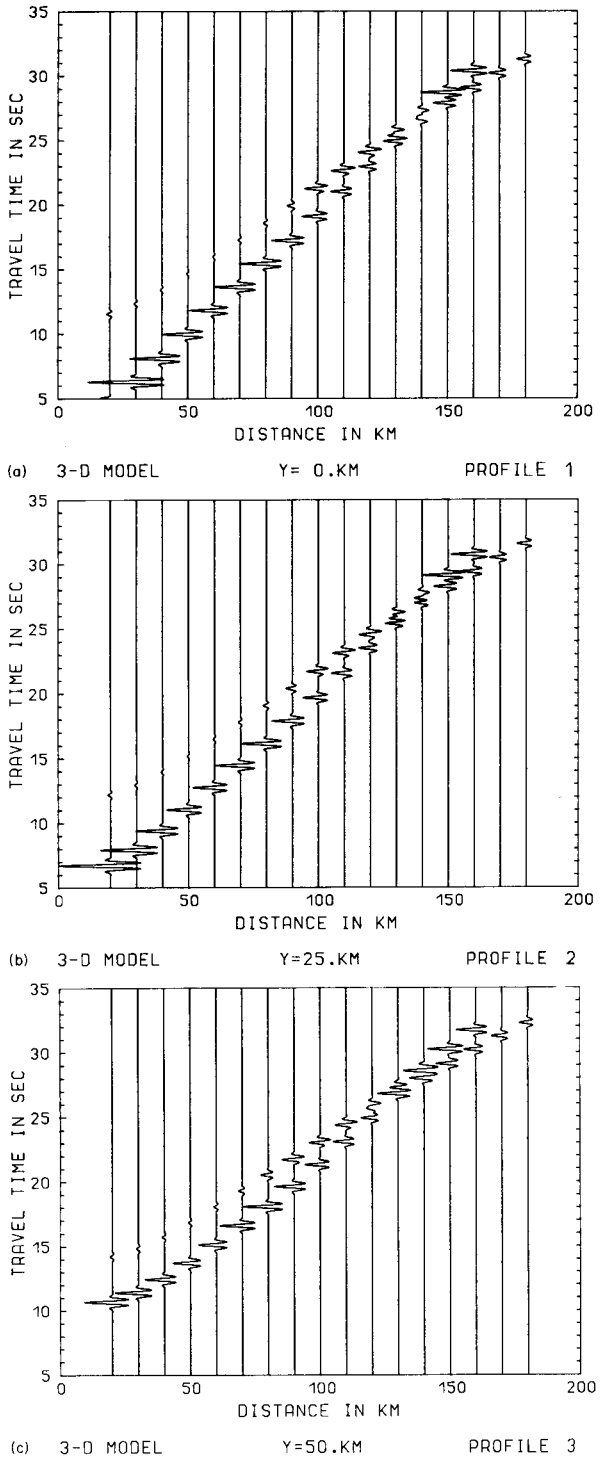

Figure 5. Synthetic seismograms of the vertical component of the displacement vector of the *P*-waves propagating in the model shown in Fig. 2. The seismograms are computed along the profiles depicted in Figs 3 and 4. The horizontal axes are labelled by the corresponding x-coordinates. The prevailing frequency is 2 Hz, $\gamma = 4$, $\nu = 0$. No reduction of time axes, no scaling of amplitudes.

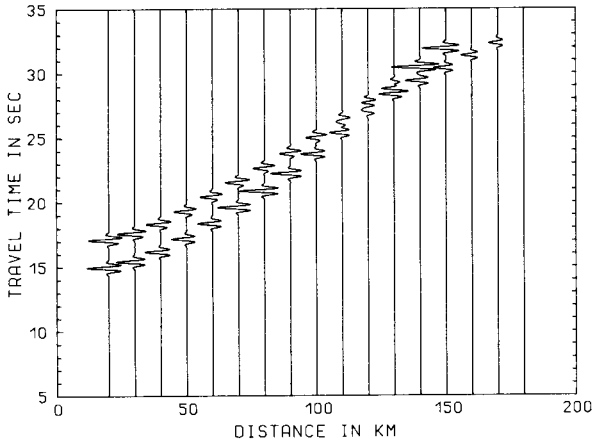

(d) 3-D MODEL Y=75.KM PROFILE 4

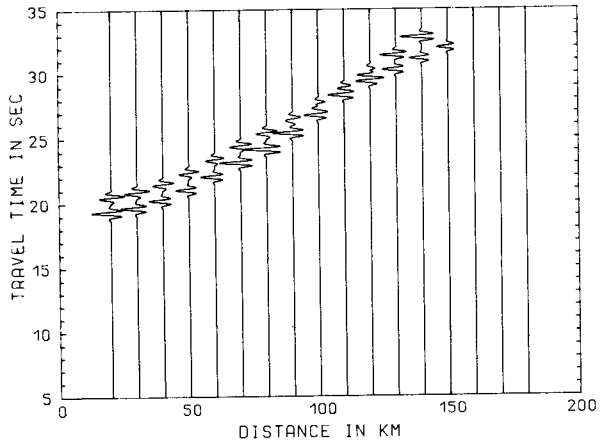

(e) 3-D MODEL Y=100.KM PROFILE 5

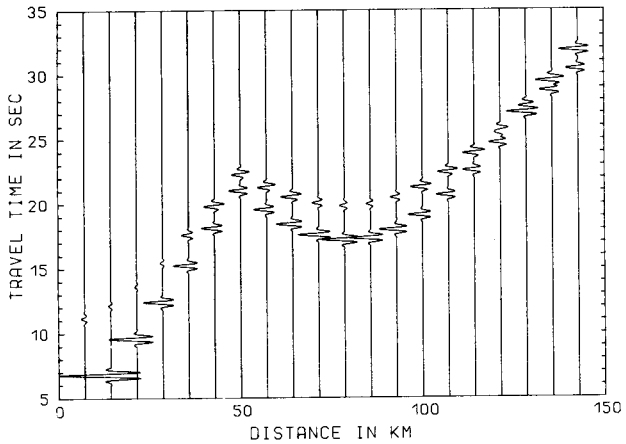

(f) 3-D MODEL PROFILE 6

Figure 5 – *continued*

7 Numerical examples

Several theoretical models of 3-D, but also of 2-D and 1-D, structures have been used to test the RD83 program and compare its results with the results of other programs, see, e.g. Červený & Klimeš (1984). Some synthetic seismograms for 3-D, laterally varying, layered structures have already been presented by Červený, Klimeš & Pšenčík (1982).

Here we consider a simple 3-D model of a laterally varying structure composed of two layers. The velocity distribution in two plane vertical sections for $y = 0$ and 100 km is shown in Fig. 2.

The point source of P-waves, with properties described in the previous section, is situated at the origin of the Cartesian coordinate system. The parameters of the source-time function (24) are $f_0 = 2$ Hz, $\gamma = 4$, $\nu = 0$.

Only three types of unconverted P-waves are considered in the computations: the waves refracted in the first (upper) layer ($P10$) and in the second layer ($P11P21P10$), and the wave reflected from the interal interface ($P11P10$). The termination points of the rays of the three waves at the Earth's surface are depicted in Fig. 3. The rays are specified at the source by the azimuth ϕ and declination δ. The increments $\Delta\phi$ and $\Delta\delta$ are constant in individual specified intervals, the boundaries between the intervals can be seen in the maps of the termination points in Fig. 3. The sharp increase in the density of the rays of wave $P10$ at epicentral distances of about 140 km is not caused by a change of $\Delta\delta$, but by the velocity inhomogeneities.

There are two possible errors in determining the boundaries of illuminated regions of individual elementary waves. The first of them depends on the density of rays in the vicinity of the boundary. The error is small in the region with a large density of ray termination points (small geometrical spreading). As an example, see the map of the termination points of wave $P10$ in Fig. 3. On the contrary, the error may be larger in regions with a low density of the ray termination points (high geometrical spreading), see the maps of their termination points of waves $P11P21P10$ and $P11P10$ in Fig. 3. In all the cases, this error is approximately proportional to the initial increments $\Delta\phi$ and $\Delta\delta$. It is usually small in the case of large amplitudes, but may be larger in the case of low amplitudes (high geometrical spreading).

The other error is caused by the numerical identification of the boundary of the shadow zone and does not exceed the quantity ϵ specified in the input data, described above. It would be suitable to determine ϵ inversely proportional to the density of the termination points of rays. In this case, ϵ would consistently decrease the first error. In our numerical examples, however, ϵ was chosen constant, equal to 7.5 km.

The wavefield is computed along six profiles situated on the surface (see Figs 3 and 4). Profiles 1 to 5 ($y = 0$, 25, 50, 75 and 100 km), are straight, profile 6 has a zigzag shape. The travel-time curves along these profiles, shown in Fig. 4, have been computed by the PRA (see equations 15) from the nearest termination point.

The synthetic seismograms of the vertical component of the displacement vector of P-waves along the six specified profiles are shown in Fig. 5. The horizontal axes of the sections are labelled by the corresponding x-coordinates. No reduction of time axes and no power scaling of amplitudes are applied.

The synthetic sections are self-explanatory. When the source is situated in the vertical plane containing the profile or close to it, the seismogram sections have typical features known from the modelling of seismic wave fields in 2-D laterally varying, layered structures (see Fig. 5, profiles 1 and 2). The synthetic sections, however, are rather different along the profiles distant from the source (Fig. 5, profiles 3, 4, 5) and along the zigzag profile (Fig. 5, profile 6).

Let us briefly discuss the boundaries between the illuminated and shadow regions of individual elementary waves.

The records corresponding to wave $P10$ refracted in the first layer and to reflected wave $P11P10$ are terminated at $x = 140–160$ km in the synthetic sections shown in Fig. 5. As the density of rays of wave $P10$ is very high in this region, the ray amplitudes are high and the boundary is determined very accurately, but with a systematic shift of $\epsilon = 7.5$ km into the shadow zone. Remember that the PRA does not remove the ray singularities, so that it gives a sharp termination of wave $P10$. The density of the ray termination points of reflected wave $P11P10$ close to the boundary is lower and thus the determination of the boundary is not so accurate, but this is not so important as the wave has small amplitudes and interferes there with wave $P10$.

The shadow zone of wave $P11P21P10$ at $x = 180$ km on profile 4 at $x \geqslant 160$ km on profile 5 is caused by the bottom of the model at a depth of 60 km. The error in the determination of the boundary of the shadow zone again does not exceed approximately 7.5 km, but it is not so systematic as in the case of wave $P10$. The possible errors in the determination of the boundary of the illuminated region at epicentral distances close to 100 km may be a little larger, but it is not so important because of the lower amplitudes of wave $P11P21P10$ and its interference with reflected wave $P11P10$.

Let us emphasize that the presented examples of computations are rather simple, program RD83 can be used to evaluate more complex models, with many other types of elementary waves (S, converted, multipy reflected), and for different components of the displacement vector (vertical, arbitrary horizontal). Fig. 5 was computed as a testing example of program RD83 and has only a methodical character; the amplitudes of individual waves are not quite correct due to a certain mistake in the original version of the program. This, however, does not influence any conclusion presented in this paper.

8 Conclusions

The paraxial ray approximation offers various possibilities in the computation of seismic wavefields in inhomogeneous media, which are not available in the standard ray method.

One of the most important possibilities is a fast and effective computation of travel times, ray amplitudes and synthetic seismograms in 3-D laterally varying, layered structures. The approach is especially convenient if we wish to compute synthetic seismograms along a system of profiles. It is only necessary to cover the region of the Earth's surface containing the profiles by a sufficiently dense system of ray termination points. Then the construction of seismograms at any point or along any profile in the region is very easy and inexpensive. If seismograms along a single profile are required, then it may be more convenient to use the two-point ray tracing procedure as described in Section 4.2.

For a more reliable application of the PRA, it will be very useful to determine the position of the boundaries of the regions illuminated by individual elementary waves. Such a procedure is commonly applied to 2-D computations of synthetic seismograms, see Červený and Pšenčík (1981).

If the closest ray termination point is only used for the evaluation of the wavefield at a receiver, it must be taken into account that the accuracy of the computations may be even lower than in the standard ray method. The accuracy would increase if we use a weighted superposition of paraxial approximations corresponding to several closest termination points. Such an approach is involved in the summation of Gaussian beams where the weighed function is automatically obtained and has a Gaussian form. The application of the weighted superposition would not increase the computing time very much.

References

Červený, V., 1983. Synthetic body wave seismograms for laterally varying layered structures by the Gaussian beam method, *Geophys. J. R. astr. Soc.*, **73**, 389–426.

Červený, V. & Hron, F., 1980. The ray series method and dynamic ray tracing systems for three-dimensional inhomogeneous media, *Bull. seism. Soc. Am.*, **70**, 47–77.

Červený, V., Klimeš, L & Pšenčík, I., 1982. Synthetic seismic wave fields for 2-D and 3-D inhomogeneous structures, in *Proc. 27th int. Geophys. Symp. A(I), Bratislava*, pp. 17–28, Geofyzika n.p., Brno.

Červený, V. & Klimeš, L., 1984. Synthetic body wave seismograms for three-dimensional laterally varying media, *Geophys. J. R. astr. Soc.*, **79**, 119–133.

Červený, V. & Pšenčík, I., 1981. 2-D seismic ray package, *Res. Rep.*, Institute of Geophysics, Charles University, Prague.

Červený, V. & Pšenčík, I., 1983. Gaussian beams and paraxial ray approximation in three-dimensional elastic inhomogenous media, *J. Geophys.*, **53**, 1–15.

Červený, V. & Pšenčík, I., 1984. Gaussian beams in elastic 2-D laterally varying layered structures, *Geophys. J. R. astr. Soc.*, **78**, 65–91.

Chapman, C. H. & Drummond, R., 1982. Body wave seismograms in inhomogeneous media using Maslov asymptotic theory, *Bull. seism. Soc. Am.*, **72**, 277–317.

Cline, A. K., 1981. *FITPACK – software package for curve and surface fitting employing splines under tension*, Department of Computer Science, University of Texas, Austin.

Hubral, P., 1979. A wavefront curvature approach to the computing of ray amplitudes in inhomogeneous media with curved interfaces, *Studia geophys. geod.*, **23**, 131–137.

Klimeš, L., 1982. Mathematical modelling of seismic wave fields in 3-D laterally inhomogeneous media, *Res. Rep. No. 63*, Institute of Geophysics, Charles University, Prague (in Czech.).

Klimeš, L., 1984. Expansion of a high-frequency time-harmonic wavefield given on an initial surface into Gaussian beams, *Geophys. J. R. astr. Soc.*, **79**, 105–118.

Popov, M. M. & Pšenčík, I., 1978. Computation of ray amplitudes in inhomogeneous media with curved interfaces, *Studia geophys. geod.*, **22**, 248–258.

Pšenčík, I., 1979. Ray amplitudes of compressional, shear and converted seismic body waves in 3D laterally inhomogeneous media with curved interfaces, *J. Geophys.*, **45**, 381–390.